

# Analyses of Divertor Regimes in NSTX

*V.A. Soukanovskii, R. Maingi, C. Bush, S.F. Paul, J.  
Boedo, R. Kaita, H.W. Kugel, B.P. Le Blanc, G.D. Porter,  
A.L. Roquemore, N.S. Wolf*

This article was submitted to the 16<sup>th</sup> International Conference on  
Plasma Surface Interactions, Portland, Maine, May 24-28, 2004

**May 2004**

U.S. Department of Energy

Lawrence  
Livermore  
National  
Laboratory

## DISCLAIMER

This document was prepared as an account of work sponsored by an agency of the United States Government. Neither the United States Government nor the University of California nor any of their employees, makes any warranty, express or implied, or assumes any legal liability or responsibility for the accuracy, completeness, or usefulness of any information, apparatus, product, or process disclosed, or represents that its use would not infringe privately owned rights. Reference herein to any specific commercial product, process, or service by trade name, trademark, manufacturer, or otherwise, does not necessarily constitute or imply its endorsement, recommendation, or favoring by the United States Government or the University of California. The views and opinions of authors expressed herein do not necessarily state or reflect those of the United States Government or the University of California, and shall not be used for advertising or product endorsement purposes.

This is a preprint of a paper intended for publication in a journal or proceedings. Since changes may be made before publication, this preprint is made available with the understanding that it will not be cited or reproduced without the permission of the author.

This report has been reproduced  
directly from the best available copy.

Available to DOE and DOE contractors from the  
Office of Scientific and Technical Information  
P.O. Box 62, Oak Ridge, TN 37831  
Prices available from (423) 576-8401  
<http://apollo.osti.gov/bridge/>

Available to the public from the  
National Technical Information Service  
U.S. Department of Commerce  
5285 Port Royal Rd.,  
Springfield, VA 22161  
<http://www.ntis.gov/>

OR

Lawrence Livermore National Laboratory  
Technical Information Department's Digital Library  
<http://www.llnl.gov/tid/Library.html>

V. A. Soukhanovskii <sup>a,1</sup>, R. Maingi <sup>b</sup>, C. Bush <sup>b</sup>, S. F. Paul <sup>c</sup>,  
J. Boedo <sup>d</sup>, R. Kaita <sup>c</sup>, H. W. Kugel <sup>c</sup>, B. P. LeBlanc <sup>c</sup>,  
G. D. Porter <sup>a</sup>, A. L. Roquemore <sup>c</sup>, N. S. Wolf <sup>a</sup>,  
and NSTX Research Team

<sup>a</sup>*Lawrence Livermore National Laboratory, Livermore, CA, USA*

<sup>b</sup>*Oak Ridge National Laboratory, Oak Ridge, TN, USA*

<sup>c</sup>*Princeton Plasma Physics Laboratory, Princeton, NJ, USA*

<sup>d</sup>*University of California at San Diego, La Jolla, CA, USA*

## Analyses of divertor regimes in NSTX

---

### Abstract

Identification of divertor operating regimes is of particular importance for heat and particle control optimization in high performance plasmas of a spherical torus, because of the magnetic geometry effects and compactness of the divertor region. Recent measurements of radiated power, heat and particle fluxes in lower single null and double null plasmas with 0.8 – 6 MW NBI heating suggest that the inner divertor is detached at  $\bar{n}_e \leq 2 - 3 \times 10^{19} \text{ m}^{-3}$  whereas the outer divertor is attached, operating in the high recycling regime. This resilient state exists in most L- and H-mode plasmas. The inner divertor transiently re-attaches in ELMy H-mode plasmas when heat pulses from type I or type III ELMs hit the divertor.

*Key words:* spherical torus, divertor, detachment, fueling

*PACS:* 52.40.Hf, 52.55.Hc, 52.55.Dy

*JNM keywords:* I0100 Impurities, P0500 Plasma-Materials Interactions, P0600

*Plasma Properties, S1300 Surface Effects*

*PSI-16 keywords:* Divertor plasma, divertor modeling, NSTX, recycling, UEDGE

---

---

<sup>1</sup> Email address: vlad@llnl.gov

## 1 Introduction

Identification of divertor operating regimes is of particular importance for heat load and particle control optimization in high performance plasmas of a spherical torus (ST). Based on the ability of a divertor to sustain a parallel temperature gradient and effectively dissipate the heat load, three divertor operating regimes have been observed in large aspect ratio tokamaks: a sheath-limited, a high-recycling and a detached regime. Present understanding of the divertor regimes relies on the physics of parallel and perpendicular heat and particle transport, particle drifts, and neutral transport [1], and the studies of the ST geometry implications have just begun [2]. Both the magnetic geometry effects, such as low toroidal field, short connection lengths, large flux expansion ratio, large mirror ratio, and the compactness of the divertor region are the factors which may affect the boundaries of the divertor regimes in the plasma operating space. Progress towards an L-mode plasma regime with a detached divertor has been made in the MAST spherical tokamak [3]. Observations of the sheath-limited and high-recycling regimes and the simultaneous inner and outer divertor detachment in a balanced double-null configuration have been reported at core plasma densities exceeding the Greenwald limit and neutral beam injection (NBI) power  $P_{NBI} \leq 0.75$  MW. General similarities in divertor regimes between MAST and large aspect ratio tokamaks have been observed, except that the detachment would take place at very low target  $n_t \simeq 2-3 \times 10^{18} \text{ m}^{-3}$ . This article reports on the first results from divertor regime studies in the National Spherical Torus Experiment (NSTX).

## 2 Experiment

NSTX is a medium-size low aspect ratio device ( $A \geq 1.27$ ,  $R = 0.85$  m,  $a = 0.67$  m). Long pulse  $t \leq 1$  s L- and H-mode plasmas are a standard operating regime. The analyzed pulse conditions comprised typical  $I_p = 0.8 - 1.0$  MA,  $B_t \leq 0.45$  T plasmas heated by 0.8 - 6 MW neutral beams with  $T_e(0) \simeq (0.8 - 1.0)$  keV,  $\bar{n}_e \simeq (2 - 5) \times 10^{19} \text{ m}^{-3}$ ,  $Z_{eff}(0) < 2$ ,  $\tau_E^L \simeq 50 - 100$  ms. A lower single null (LSN) magnetic configuration was utilized with the *drsep* parameter of -1.5 cm (Fig. 1), the ion  $\nabla B$  drift toward the lower X-point, the elongation of  $\kappa = 1.6 - 2.2$ , triangularity of  $\delta = 0.3 - 0.4$ ,  $q_{95} \simeq 6 - 7$ , the X-point height of 15 - 20 cm, and the flux expansion (evaluated at outer strike point) of 3 to 4. The deuterium plasmas were fueled by injecting gas from both a low field side (LFS) injector at about 120 Torr l/s from and a center-stack high field side (HFS) injector at the decreasing rate from 80 to 10 Torr l/s. Whereas this fueling scheme allowed better access to the H-modes, the  $\bar{n}_e$  increased continuously and non-disruptively at a rate of  $S \leq 20$  Torr l/s [4]. NSTX divertor has an open geometry. The center column, divertor

plates and passive plates are covered with CFC and ATJ graphite tiles 1" and 2" thick. Data from several edge diagnostics shown in Fig. 1 have been used in the present analysis. Experimental divertor physics is inherently two dimensional. Edge and divertor diagnostics in NSTX are point-localized or one dimensional, making the present analysis dependent on the modeling and extrapolation assumptions. Divertor infra-red emissivity profiles are recorded by a 30 Hz infra-red camera, and radial heat flux profiles were inferred using the one dimensional (1D) heat conduction model of the ATJ graphite tiles [5]. Divertor  $D_\alpha$ ,  $D_\gamma$  and inboard mid-plane  $D_\alpha$  brightness profiles are recorded by photometrically calibrated spectrally filtered 1D CCD arrays [6]. Outer mid-plane edge and scrape-off layer (SOL) temperature and density were measured by the Multi-point Thomson scattering system with 2-3 cm spatial resolution. Four chord divertor bolometry system and tile-mounted divertor Langmuir probes have recently come on-line and the first results are used in the analysis. Magnetic equilibrium is calculated using the EFIT code.

### 3 Results and discussion

Despite vast differences in the core and edge power and density operational space of the L- and H-mode LSN plasmas [7],[8], one resilient divertor state, referred here as the IDOA (inner detached, outer attached) state, dominates the operational space. Edge power, recycling and neutral flux measurements in NSTX have been previously reported [7], [9]. We note that the  $D_\alpha$  brightness reported in the latter reference must be multiplied by a factor of 51 due to a calibration problem. In general, initial results from the divertor power balance indicate that power accounting in NSTX is fairly good: up to 50 % of the input power reaches the divertor as heat, up to 10 % is radiated in the core plasma, and up to 10 % is radiated in the divertor [10]. Particle balance indicates that the wall is in a pumping state [11], as a result of an effective wall conditioning program on NSTX [12]. To illustrate the IDOA state features, we use an L-mode discharge for which an extended set of diagnostics is available (Fig. 2). The LFS gas feed starts at 0.09 s. A sign of the inner divertor detachment is the increase of the  $D_\gamma/D_\alpha$  brightness ratio. The ratio has been used to identify volume recombination which occurs at  $T_e \leq 5$  eV and is correlated with an onset of detachment [13]. At the same time, the inner divertor Langmuir probe P3 measures a sharp decrease in the ion saturation current, whereas the P1 probe current increases, consistent with the detached plasma region extending upwards. The outer divertor plate probe saturation currents (e.g. P4) increase gradually indicating the outer strike point drift toward the probe. An increase of divertor radiated power is also apparent on the two lower chords of the bolometer system B1 and B2. Figure 3 shows the  $D_\alpha$ ,  $D_\gamma$  and  $q_t$  profiles at the times  $t = 0.19$  s and  $0.26$  s. The shown profiles are typical for the IDOA state.

The inner divertor heat flux being already low gradually decreases beyond the IR camera detectability threshold. The Balmer  $\gamma$  emission in the inner divertor is present only when the  $D_\alpha$  in-out asymmetry is  $A \geq 1$ . Whereas the present data set is somewhat limited in spatial resolution, it is suggestive of the *partial* divertor detachment observed in tokamaks [14].

We now summarize the heat flux and recycling trends measured in the plasmas with the IDOA divertor. Heat fluxes up to  $10 \text{ MW/m}^2$  have been measured in NSTX. Peak heat flux is a non-linear function of input power for  $P_{in} = 2 - 6 \text{ MW}$ . As in conventional tokamaks higher outboard peak heat fluxes are measured in the L-mode, whereas the inboard heat loads are  $q_{in} \leq 1 \text{ MW/m}^2$ , being similar in the H- and L-modes, apparently leading to the observed divertor similarities. Inboard and outboard heat fluxes are found to be independent of the the gas fueling location for both the low and high field side gas injectors. This suggests that the NSTX divertor regimes are not affected by the rate of gas puffing  $S = 20 - 120 \text{ Torr l / s}$ . The average inboard heat flux is a factor of 2 - 3 lower than the outboard, whereas the ratio is about 4 - 5 for the peak heat flux [7]. Divertor recycling measurements also indicate many similarities in  $(P_{in}, n_e)$  space. The  $D_\alpha$  brightness in the inner and outer divertor increases with power in L- and H-mode plasmas. The divertor  $D_\alpha$  brightness is almost always higher in L-mode vs H-mode plasmas, although the inner divertor brightness is comparable at  $\bar{n}_e \geq 3 \times 10^{19} \text{ m}^{-3}$ . The in-out  $D_\alpha$  peak brightness asymmetry  $A_{D_\alpha} = B_{in}/B_{out}$  develops due to a much faster increase of the inboard emission with  $\bar{n}_e$ . The asymmetry is 4 - 6 in the L-mode, and up to 15 in the H-mode plasmas. It is, however, smaller than or about 1 at low densities, and greater than 1 at  $\bar{n}_e \simeq 2.5 \times 10^{19} \text{ m}^{-3}$  in the L-mode, and at slightly higher  $\bar{n}_e$  in the H-mode [9]. The asymmetry is always  $A \leq 1 - 1.5$  in ohmic plasmas with  $P_{in} \leq 0.7 \text{ MW}$ . The asymmetry in recycling has been observed in large aspect ratio tokamaks, and in many cases is attributed to the inner divertor detachment, in some instances accompanied by an X-point MARFE [15], [16]. Several factors, which can be at play simultaneously, may contribute to the development of the recycling asymmetry: the temperature and density dependence of atomic rates [13], different inner and outer flux tube lengths [17], and the radial  $E \times B$  drift [18]. The latter can be substantial in the recycling (high density) regime, resulting in a high drift velocity directed toward the inner target for  $\nabla B$  toward the lower X-point. In NSTX we attribute the large asymmetry ( $A > 2$ ) to the inner divertor detachment. The asymmetry can be explained by comparing the calculated deuterium Balmer  $\alpha$  emissivity rates [13] for the  $T_e \simeq 2 - 5 \text{ eV}$ ,  $n_e \leq 10^{20} \text{ m}^{-3}$  recombining plasmas and the  $T_e \simeq 10 - 30 \text{ eV}$ ,  $n_e \leq 5 \times 10^{19} \text{ m}^{-3}$  ionizing plasmas. Another supporting factor for this notion is the lower divertor recycling behavior in the ELMy H-mode plasmas. The IDOA divertor state is resilient to the impact of ELMs. H-mode plasma regimes with type I, type III, and type V ELMs have been identified in NSTX [19]. When the type I and III ELMs ( $0.01 < \Delta W/W < 0.30$ , where  $W$  is the plasma stored

energy) reach the lower divertor the recycling profile asymmetry transiently reverses ( $A < 1$ ), and recovers between ELMs (Fig. 4), suggestive of a transient re-attachment of the detached inner divertor as the heat flux is transiently increased during the ELM heat pulse. Similar recycling behavior has been reported in large aspect ratio tokamaks [15].

Since the direct  $T_e, n_e$  divertor measurements are not yet available in NSTX, the two point model (2PM) of the scrape-off layer (SOL) transport [1] is used to estimate plasma conditions in the divertor. The 2PM relates the plasma parameters at the divertor target  $T_t, n_t, \Gamma_t$  to the "upstream" parameters through the Spitzer heat conduction equation, the pressure balance in a flux tube, and the sheath condition at the target surface [1]. The 2PM does not include the radiation effects and any ST relevant factors. The measured outer mid-plane SOL  $T_e^{sep} \simeq 20 - 40$  eV and  $n_e^{sep} \simeq 2 - 7 \times 10^{18} \text{ m}^{-3}$  yield the SOL collisionality  $\nu_e^* \geq 3$ , suggesting that the outer divertor is in the high recycling regime. The 2PM predicts  $T_t^{out} \leq 30$  eV,  $n_t^{out} \leq 7 \times 10^{18} \text{ m}^{-3}$  for the outer divertor if the measured heat flux density  $q_{in} \leq 6 \text{ MW/m}^2$  and the connection length of  $L_c \simeq 30$  m are used. For the inner divertor parameters  $q_{in} \leq 1 \text{ MW/m}^2$ ,  $L_c \leq 30$  this estimate yields  $T_t^{in} \simeq 1 - 7$  eV,  $n_t^{in} \leq 8 \times 10^{19} \text{ m}^{-3}$ . The estimates suggest that the inner target may be detached, whereas the outer target operates in the flux limited (high-recycling) regime. Peak  $D_\alpha$  behavior and the divertor  $D_\alpha$  in-out asymmetry also support this notion, as  $n_t \sim n_u^3$ ,  $T_t \sim n_u^{-2}$  in the high-recycling regime, whereas  $T_t$  decreases and  $n_t$  increases as the detachment occurs, leading to the observed increase in  $D_\alpha$  intensity. To put our analyses on a firm theoretical ground numerical modeling efforts have been on-going. The multi-fluid code UEDGE with purely diffusive and diffusive-convective models is used. The modeling has not been able to accurately reproduce the observed recycling asymmetry, and moderate success was claimed in matching the edge  $T_e, n_e$  profiles and divertor heat fluxes [20]. Nevertheless, the modeling is very useful in guiding experimental work. An example of this is shown in Fig. 5: UEDGE with an anomalous diffusive radial transport model is used to estimate the detachment boundaries [21]. Input power and electron density at the core boundary ( $\psi_N = 0.9$ ) are systematically varied using an H-mode LSN equilibrium and measured edge profiles. The model includes carbon impurities with the source determined by physical and chemical sputtering from all plasma facing surfaces. Two criteria for divertor detachment are used: the decrease of peak divertor  $T_e$  to 5 eV or less, and the saturation of the total ion current to the plate as the upstream density is increased. The two criteria have led to similar results and correctly predicted the onset of the IDOA state. However, the observed IDOA divertor boundaries are much wider, the inner divertor is attached in ohmic ( $P_{in} \leq 0.7 \text{ MW}$ ) and low density plasmas, and the outer divertor detachment has not been observed even in plasmas with  $n_e(\psi_{90}) \leq 6 \times 10^{19} \text{ m}^{-3}$ .

In summary, present experimental results suggest that some features of NSTX

divertor operation are similar to high recycling and detached divertors of large aspect ratio tokamaks. Due to a strong heat flux dispersal in the inner divertor in the L- and H-mode plasmas ( $q_t \leq 1 \text{ MW/m}^2$ ) the inner divertor operates in a detached state at  $\bar{n}_e \geq 2 - 3 \times 10^{19} \text{ m}^{-3}$  ( $0.2 \leq \bar{n}_e/n_G \leq 0.9$ ),  $P_{in} = 1.5 - 7 \text{ MW}$ , whereas the outer divertor is attached. Future experiments will explore the divertor operational space further, attempting to produce a fully detached radiative divertor by increasing the core density and edge radiated power, and studying the role of impurities and electromagnetic drifts in the detachment process.

## Acknowledgments

The authors thank D. Gates, D. Mueller, and T. Stevenson (PPPL) for operating the NSTX device, and S. Sabbagh (Columbia University) for EFIT magnetic equilibrium reconstructions. This research was supported by the U.S. Department of Energy under contracts No. W-7405-Eng-48, DE-AC02-76CH03073, DE-AC05-00OR22725.

This work was performed under the auspices of the U. S. Department of Energy by the University of California, Lawrence Livermore National Laboratory under Contract No. W-7405-Eng-480

## References

- [1] P. C. Stangeby, The plasma boundary of Magnetic Fusion Devices, IoP Publishing, Bristol and Philadelphia, 2000.
- [2] A. Kirk, W. Fundamenski, J.-W. Ahn, G. Counsell, Plasma Phys. Control. Fusion 45 (8) (2003) 1445–1463.
- [3] G. Counsell, J.-W. Ahn, R. Cohen, A. Kirk, P. Helander, R. Martin, D. Ryutov, A. Tabasso, H. Wilson, Y. Yang, the MAST team, Nuc. Fusion 43 (10) (2003) 1197–1203.
- [4] R. Maingi, C. S. Chang, S. Ku, T. Biewer, R. Maqueda, M. Bell, R. Bell, C. Bush, D. Gates, S. Kaye, H. Kugel, B. LeBlanc, J. Menard, D. Mueller, R. Raman, S. Sabbagh, V. Soukhanovskii, the NSTX Team, Plasma Phys. Control. Fusion 46 (5A) (2004) A305–A313.
- [5] R. Maingi, H. W. Kugel, C. J. Lasnier, A. L. Roquemore, V. A. Soukhanovskii, C. E. Bush, J. Nuc. Mater. 313 (2003) 1005.
- [6] V. A. Soukhanovskii, A. L. Roquemore, C. H. Skinner, D. Johnson, R. Maingi, C. Bush, F. Paoletti, S. Sabbagh, Rev. Sci. Instrum. 74 (2003) 2094.
- [7] R. Maingi, M. Bell, R. Bell, C. Bush, E. Fredrickson, D. Gates, T. Gray, D. Johnson, R. Kaita, S. Kaye, S. Kubota, H. Kugel, C. Lasnier, B. LeBlanc, R. Maqueda, D. Mastrovito, J. Menard, D. Mueller, M. Ono, F. Paoletti,



- S. Paul, Y.-K. Peng, A. Roquemoire, S. Sabbagh, C. Skinner, V. Soukhanovskii, D. Stutman, D. Swain, E. Synakowski, T. Tan, J. Wilgen, S. Zweben, *Nuc. Fusion* 43 (9) (2003) 969–974.
- [8] R. Maingi, M. G. Bell, R. E. Bell, J. Bialek, C. Bourdelle, C. E. Bush, D. S. Darrow, E. D. Fredrickson, D. A. Gates, M. Gilmore, T. Gray, T. R. Jarboe, D. W. Johnson, R. Kaita, S. M. Kaye, S. Kubota, H. W. Kugel, B. P. LeBlanc, R. J. Maqueda, D. Mastrovito, S. S. Medley, J. E. Menard, D. Mueller, B. A. Nelson, M. Ono, F. Paoletti, H. K. Park, S. F. Paul, T. Peebles, Y.-K. M. Peng, C. K. Phillips, R. Raman, A. L. Rosenberg, A. L. Roquemoire, P. M. Ryan, S. A. Sabbagh, C. H. Skinner, V. A. Soukhanovskii, D. Stutman, D. W. Swain, E. J. Synakowski, G. Taylor, J. Wilgen, J. R. Wilson, G. A. Wurden, S. J. Zweben, the NSTX Team, *Plasma Phys. Control. Fusion* 45 (5) (2003) 657–669.
- [9] V. A. Soukhanovskii, R. Maingi, R. Raman, H. W. Kugel, B. P. LeBlanc, A. L. Roquemoire, C. Lasnier, in: R. Koch, S. Lebedev (Eds.), *Proceedings of the 30th EPS Conference on Plasma Physics and Controlled Fusion*, St. Petersburg, Russia, 2003.
- [10] S. Paul et. al., These proceedings .
- [11] V. A. Soukhanovskii, R. Maingi, R. Raman, H. W. Kugel, B. P. LeBlanc, A. L. Roquemoire, C. H. Skinner, *J. Nuc. Mater.* 313 (2003) 573.
- [12] H. W. Kugel, V. A. Soukhanovskii, M. Bell, W. Blanchard, D. Gates, B. LeBlanc, R. Maingi, D. Muller, H. K. Na, S. Paul, C. H. Skinner, D. Stutman, W. R. Wampler, *J. Nuc. Mater.* 313-316 (2003) 187.
- [13] G. M. McCracken, M. F. Stamp, R. D. Monk, A. G. Meigs, J. Lingertat, R. Prentice, A. Starling, R. J. Smith, A. Tabasso, *Nuc. Fusion* 38 (4) (1998) 619.
- [14] T. Petrie, D. Hill, S. Allen, N. Brooks, D. Buchenauer, J. Cuthbertson, T. Evans, P. Ghendrih, C. Lasnier, A. Leonard, R. Maingi, G. Porter, D. Whyte, R. Groebner, R. Jong, M. Mahdavi, S. Thompson, W. West, R. Wood, *Nuc. Fusion* 37 (3) (1997) 321–338.
- [15] A. Loarte, R. Monk, J. Martín-Solís, D. Campbell, A. Chankin, S. Clement, S. Davies, J. Ehrenberg, S. Erents, H. Guo, P. Harbour, L. Horton, L. Ingesson, H. Jäckel, J. Lingertat, C. Lowry, C. Maggi, G. Matthews, K. McCormick, D. O’Brien, R. Reichle, G. Saibene, R. Smith, M. Stamp, D. Stork, G. Vlases, *Nuc. Fusion* 38 (3) (1998) 331–371.
- [16] A. Hatayama, H. Segawa, N. Komatsu, R. Schneider, D. P. Coster, N. hayashi, S. sakurai, N. Asakura, *J. Nuc. Mater.* 290-293 (2001) 407.
- [17] U. Wenzel, D. Coster, A. Kallenbach, H. Kastelewicz, M. Laux, H. Maier, R. Schneider, A. U. Team, *Nuc. Fusion* 41 (11) (2001) 1695–1701.
- [18] P. Stangeby, A. Chankin, *Nuc. Fusion* 36 (7) (1996) 839–852.
- [19] R. Maingi et. al., These proceedings .

- [20] A. Yu. Pigarov (UCSD) and G. D. Porter (LLNL), Personal communication .
- [21] N. S. Wolf, G. D. Poter, D. N. Hill, S. L. Allen, J. Nuc. Mater. 266-269 (1999) 739.

## List of Figures

1	Schematic of NSTX cross-section with a lower single null plasma and the diagnostics arrangement	10
2	Time traces of a representative L-mode discharge. (a) - Plasma current, input NBI power, (b) line averaged density and gas input, (c) divertor $D_\gamma/D_\alpha$ ratio, (d) divertor bolometers, (e) Ion saturation currents, (f) Strike point major radii from EFIT. Bolometer and probe notations are as in Fig. 1	11
3	Divertor $D_\alpha$ , $D_\gamma$ , and heat flux profiles for the L-mode discharge shown in Fig. 2 at times $t = 0.19$ s and $0.28$ s	12
4	Example of the reversal of the divertor recycling in-out asymmetry in double null ELMy H-mode plasma. Transient asymmetry drops to $A \leq 1$ occur when ELMs reach the divertor and the inner divertor leg re-attaches.	13
5	Divertor detachment mapping in the $(P_{in} - n_e)$ space predicted by UEDGE using the $T_e \leq 5$ eV and $I_{sat}$ criteria (red and blue lines)	14

## Figures

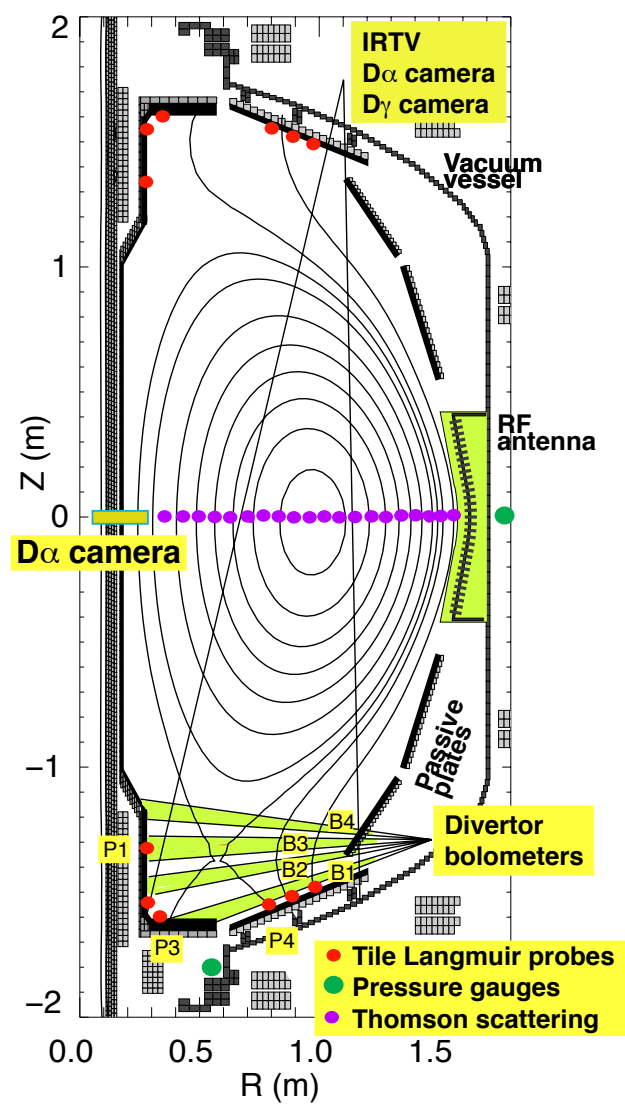


Fig. 1. Schematic of NSTX cross-section with a lower single null plasma and the diagnostics arrangement

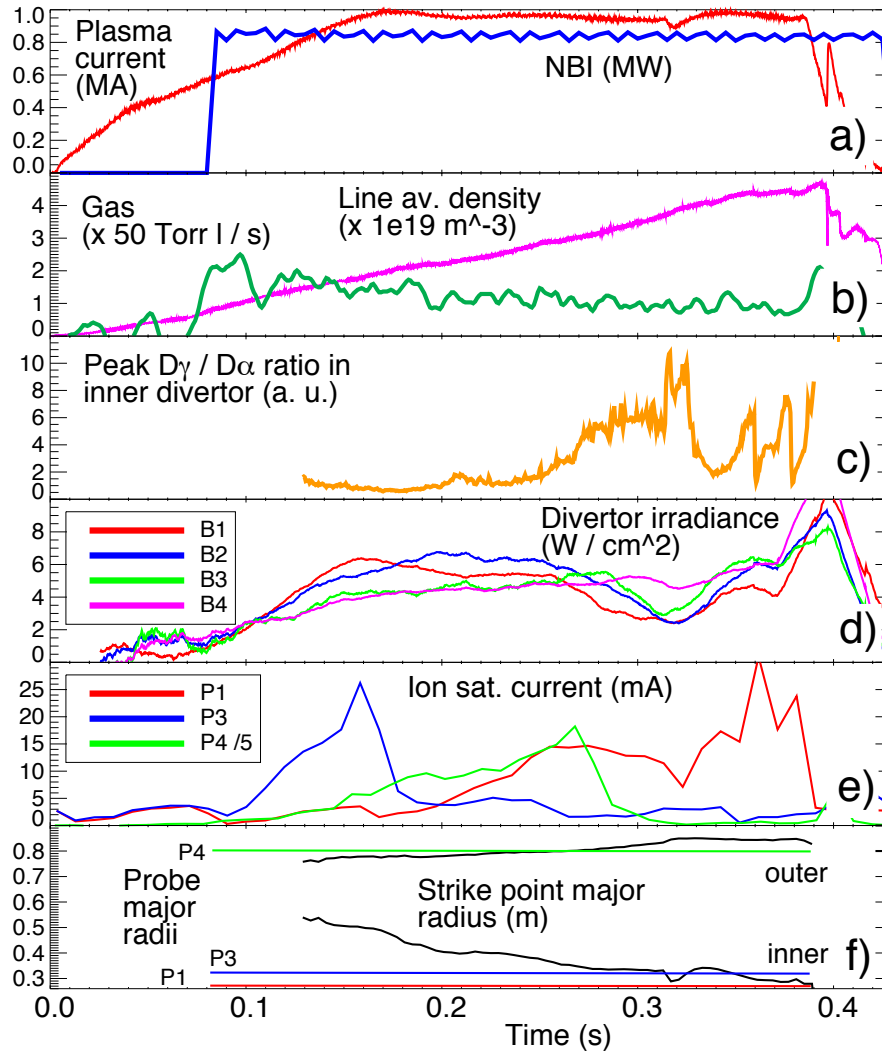


Fig. 2. Time traces of a representative L-mode discharge. (a) - Plasma current, input NBI power, (b) line averaged density and gas input, (c) divertor  $D_{\gamma}/D_{\alpha}$  ratio, (d) divertor bolometers, (e) Ion saturation currents, (f) Strike point major radii from EFIT. Bolometer and probe notations are as in Fig. 1

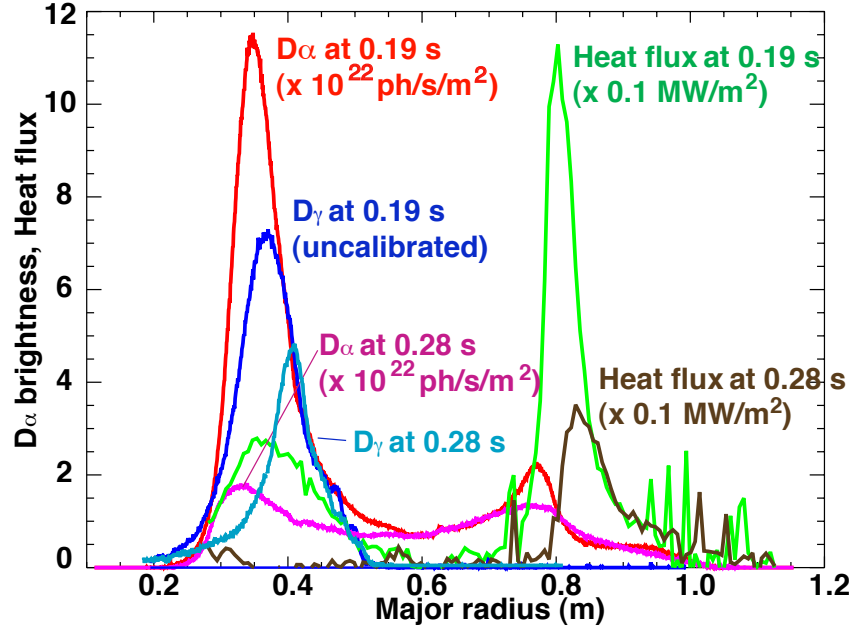


Fig. 3. Divertor  $D_\alpha$ ,  $D_\gamma$ , and heat flux profiles for the L-mode discharge shown in Fig. 2 at times  $t = 0.19$  s and 0.28 s

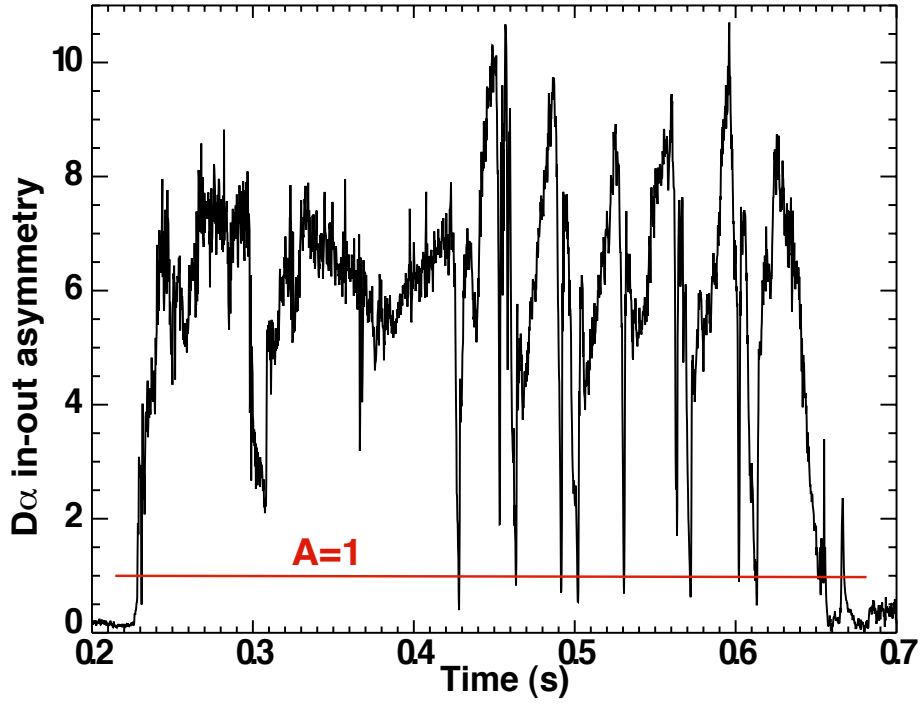


Fig. 4. Example of the reversal of the divertor recycling in-out asymmetry in double null ELMy H-mode plasma. Transient asymmetry drops to  $A \leq 1$  occur when ELMs reach the divertor and the inner divertor leg re-attaches.

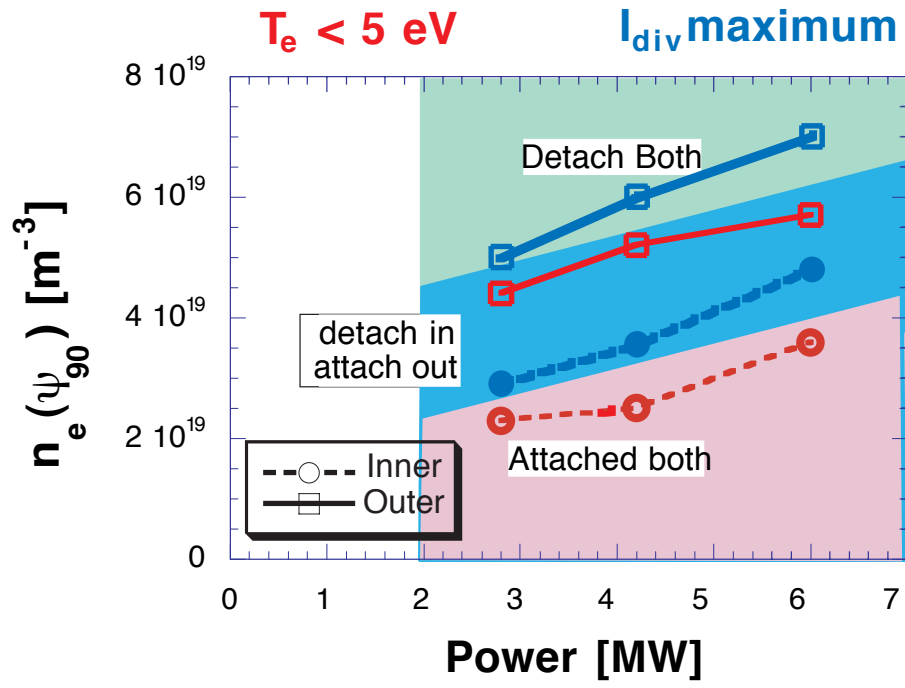


Fig. 5. Divertor detachment mapping in the  $(P_{in} - n_e)$  space predicted by UEDGE using the  $T_e \leq 5 \text{ eV}$  and  $I_{sat}$  criteria (red and blue lines)



University of California  
Lawrence Livermore National Laboratory  
Technical Information Department  
Livermore, CA 94551

